HEPATOLOGY
Official Journal of the American Association for the Study of Liver Diseases

Conjugated Bile Acids Promote Cholangiocarcinoma Cell Invasive Growth Through Activation of Sphingosine 1-Phosphate Receptor 2

Runping Liu,[1,2]* Renping Zhao,[1,2]* Xiqiao Zhou,[1,3] Xiuyin Liang,[1] Deanna J.W. Campbell,[5] Xiaoxuan Zhang,[1,2] Luyong Zhang,[1] Ruihua Shi,[3] Guangji Wang,[2] William M. Pandak,[4] Alphonse E. Sirica,[5]** Phillip B. Hylemon,[1,4]** and Huiping Zhou[1,4,6]**

Cholangiocarcinoma (CCA) is an often fatal primary malignancy of the intra- and extrahepatic biliary tract that is commonly associated with chronic cholestasis and significantly elevated levels of primary and conjugated bile acids (CBAs), which are correlated with bile duct obstruction (BDO). BDO has also recently been shown to promote CCA progression. However, whereas there is increasing evidence linking chronic cholestasis and abnormal bile acid profiles to CCA development and progression, the specific mechanisms by which bile acids may be acting to promote cholangiocarcinogenesis and invasive biliary tumor growth have not been fully established. Recent studies have shown that CBAs, but not free bile acids, stimulate CCA cell growth, and that an imbalance in the ratio of free to CBAs may play an important role in the tumorigenesis of CCA. Also, CBAs are able to activate extracellular signal-regulated kinase (ERK)1/2- and phosphatidylinositol-3-kinase/protein kinase B (AKT)-signaling pathways through sphingosine 1-phosphate receptor 2 (S1PR2) in rodent hepatocytes. In the current study, we demonstrate S1PR2 to be highly expressed in rat and human CCA cells, as well as in human CCA tissues. We further show that CBAs activate the ERK1/2- and AKT-signaling pathways and significantly stimulate CCA cell growth and invasion *in vitro*. Taurocholate (TCA)-mediated CCA cell proliferation, migration, and invasion were significantly inhibited by JTE-013, a chemical antagonist of S1PR2, or by lentiviral short hairpin RNA silencing of S1PR2. In a novel organotypic rat CCA coculture model, TCA was further found to significantly increase the growth of CCA cell spheroidal/"duct-like" structures, which was blocked by treatment with JTE-013. *Conclusion:* Our collective data support the hypothesis that CBAs promote CCA cell-invasive growth through S1PR2. (HEPATOLOGY 2014;60:908-918)

See Editorial on Page 795

Cholangiocarcinomas (CCAs) are aggressive, largely fatal primary malignancies of the intra- and extrahepatic biliary tract that, though rare, are biologically and clinically challenging because of their still poorly understood pathophysiology, high worldwide morbidity and mortality rates, and limited treatment options. Although most CCAs are sporadic and have no identifiable risk factors, chronic cholestasis and cholangitis are known to have a strong effect on

Abbreviations: 3D, three-dimensional; Ab, antibody; AKT, protein kinase B; ASBT, apical sodium-dependent bile acid transporter; BDO, bile duct obstruction; CBAs, conjugated bile acids; CCA, cholangiocarcinoma; cDNA, complementary DNA; COX-2, cyclooxygenase-2; DCA, deoxycholic acid; DMEM, Dulbecco's modified Eagle's medium; DMSO, dimethyl sulfoxide; EGFR, epidermal growth factor receptor; ERK1/2, extracellular signal-regulated kinase; FBS, fetal bovine serum; FXR, farnesoid X receptor; GAPDH, glyceraldehyde 3-phosphate dehydrogenase; GCA, glycocholic acid; GDCA, glycodeoxycholic acid; GPCRs, G-protein-coupled receptors; H&E, hematoxylin and eosin; IHC, immunohistochemistry; IL-6, interleukin-6; MAPK, mitogen-activated protein kinase; MEK, MAPK kinase; MEM, minimal essential medium; mRNA, messenger RNA; OST, organic solute transporter; PBS, phosphate-buffered saline; PSC, primary sclerosing cholangitis; PI3K, phosphatidylinositol-3-kinase; RT-PCR, reverse transcriptase polymerase chain reaction; S1P, sphingosine 1-phosphate; S1PR2, sphingosine 1-phosphate receptor 2; shRNA, short hairpin RNA; SphK1/2, sphingosine kinase 1 and 2; TCA, taurocholate; TUDCA, tauroursodeoxycholic acid; VCU, Virginia Commonwealth University.

From the [1]Department of Microbiology and Immunology, School of Medicine, Virginia Commonwealth University, Richmond, VA; [2]Key Laboratory of New Drug Screen and Drug Metabolism and Pharmacokinetics, China Pharmaceutical University, Nanjing, China; [3]Department of Gastroenterology, The First Affiliated Hospital of Nanjing Medical University, Jiangsu, China; [4]McGuire Veterans Affairs Medical Center, Richmond, VA; [5]Department of Pathology, Division of Cellular and Molecular Pathogenesis, School of Medicine, Virginia Commonwealth University, Richmond, VA; and [6]Wenzhou Medical College, Wenzhou, China.

Received October 23, 2013; accepted February 19, 2014.

CCA development and progression, as exemplified by known risk conditions predisposing for CCA, such as primary sclerosing cholangitis (PSC), hepatolithiasis, and choledocholithiasis, as well as liver fluke infestation of the biliary tract.[1-3] Bile duct obstruction (BDO) has also been recently shown, in rodent models, to be a potent promoter of CCA growth and progression.[4,5]

Clinically, CCA patients have been reported to exhibit significantly higher bile acid concentrations in bile, compared with patients with benign biliary diseases,[6,7] with BDO apparently contributing to the alterations in bile acid concentrations in CCA.[6] Moreover, taurine- and glycine-conjugated bile acids (CBAs) were found to be significantly elevated in bile of CCA patients, compared with bile from patients with benign biliary disease,[7] suggesting that elevated CBAs in bile may be playing an etiopathogenic role in human cholangiocarcinogenesis.

The role of CBAs in CCA tumorigenesis is further supported by the recent findings of Dai et al.,[8] who reported that CBAs promoted the growth of human QBC939 CCA cells *in vitro*, as well as QBC 939 CCA tumor growth *in vivo* in a mouse xenograft model, whereas free bile acids were found to be growth inhibitory. These researchers further demonstrated that CBAs enhanced the activation of nuclear factor kappa B, which was associated with an up-regulation of the expression of interleukin-6 (IL-6) and cyclooxygenase-2 (COX-2) in CCA cells, whereas free bile acids had opposite effects. Both IL-6 and COX-2 have been implicated in CCA growth and apoptosis resistance.[9,10] Furthermore, CBAs also decreased the expression of farnesoid x receptor (FXR), an important bile acid nuclear receptor and putative liver tumor suppressor, in cultured QBC939 CCA cells. In contrast, free bile acids were found to increase FXR expression in these cells. CBA-induced subcutaneous tumor growth of QBC939 CCA xenografts was significantly inhibited by the FXR agonist, GW4064, in nude mice.[11]

The sphingosine 1-phosphate (S1P) pathway has been demonstrated to contribute to the antiapoptotic effects induced by BDO in rat liver,[12] to play a role in the pathophysiology of portal hypertension in cirrhotic rats induced by BDO,[13] to be involved in mouse liver fibrogenesis and in hepatic myofibroblast motility,[14] and to be possibly involved in CCA progression, as reflected by increased tumor growth and associated malignant obstruction of the bile duct in relation to a progressive increase in tumor sphingosine kinase 1 (SphK1) expression in an orthotopic rat CCA model closely mimicking the human disease.[15] S1P elicits its biological function either as an intracellular signaling molecule or as an agonist of G-protein-coupled receptors (GPCRs).[16] More recently, we have shown that conjugated, but not unconjugated, bile acids can specifically induce extracellular signal-regulated kinase (ERK)1/2 (p42/44 mitogen-activaed protein kinase [MAPK]) and protein kinase B (AKT) signaling primarily through activation of sphingosine 1-phosphate receptor 2 (S1PR2) in primary rat hepatocytes.[17]

In an effort to gain a new mechanistic insight into the role played by CBAs as mediators of CCA growth and invasion, and based on our recent findings demonstrating CBAs to be potent inducers of ERK1/2 and AKT signaling through S1PR2 activation, we have now examined, in human and rat CCA cells, the expression and functional relationships between S1PR subtypes and their activation by CBAs in relation to CCA cell growth and migration/invasion. We further investigated the role of S1PR2 on CCA "spheroid/duct-like" growth in a novel three-dimensional (3D) organotypic rat CCA culture model. Collectively, our findings strongly suggest that S1PR2 plays a crucial role in CBA-mediated CCA cell growth and invasion.

The work was supported by the A.D. Williams Award (to H.Z.) and the National Institutes of Health (NIH) (grant no.: R01 DK-057543; to P.B. and H.Z.). This study is also partially supported by VA Merit Award 1I01BX001390 (to H.Z.), the National Science Foundation of China (grant nos.: 81070245 and 81270489; to H.Z.), and NIH grants R01CA-83650 and 5R01CA-39225 (to A.E.S.). Funding was also provided by a NIH/National Institute of Neurological Disorders and Stroke center core grant (5P30NS047463).

**These authors contributed equally to this work.*

***Drs. Zhou, Hylemon, and Sirica contributed equally to this work.*

Address reprint requests to: Huiping Zhou, Ph.D., Department of Microbiology and Immunology, Medical College of Virginia Campus, Virginia Commonwealth University, P.O. Box 908678, Richmond, VA 23298-0678. E-mail: hzhou@vcu.edu; fax: 804-828-0676.

View this article online at wileyonlinelibrary.com.

DOI 10.1002/hep.27085

Potential conflict of interest: Nothing to report.

Materials and Methods

Materials. S1P and JTE-013 (S1PR2 antagonist) were purchased from Cayman Chemical (Boston, MA). The Bio-Rad protein assay reagent, Precision Plus Protein Kaleidoscope Standards, and iQ™ SYBR® Green Supermix were obtained from Bio-Rad (Hercules, CA). IRDye secondary antibody (Ab) was from LI-COR (Lincoln, NE). FuGene HD transfection Reagent was from Promega (Madision, WI). Rat type I collagen and BD Biocoat Matrigel Invasion Chambers were from BD Biosciences (Bedford, MA). Taurocholate (TCA), tauroursodeoxycholic acid (TUDCA), glycodeoxycholic acid (GDCA), glycocholic acid (GCA), deoxycholic acid (DCA), and cell culture chemicals were from Sigma-Aldrich (St. Louis, MO).

Cell Lines. The immortalized nontumorigenic rat BDE1 cholangiocyte cell line, spontaneously transformed malignant rat BDEsp cholangiocyte cell line, BDEsp tumor-derived BDEsp-TDE_{H10} CCA cell strain (clone H10), and BDEsp tumor-derived BDEsp-TDF_{E4} cancer-associated myofibroblastic cell strain (clone E4) used in this study were cultured as described previously.[4,18] The human normal biliary epithelial cell line, H69, was obtained from Dr. Gregory J Gores (Mayo Clinic, Rochester, NY). The human CCA cell lines (HuCCT1, SG231, and CCLP1) used in our experiments were originally obtained from the Japanese Cancer Research Resources Bank. H69 cells were cultured in Dulbecco's modified Eagle's medium (DMEM)/Ham's F12 containing 10% fetal bovine serum (FBS), penicillin G (100 U/mL), streptomycin (100 μg/mL), insulin (0.1 μmol/L), epinephrine (10 μg/mL), and epidermal growth factor (EGF; 30 ng/mL). HuCCT1 cells were cultured in RPMI 1640 medium, supplemented with 10% FBS, 2 mM of L-glutamine, and 50 μg/mL of gentamicin. SG231 cells were cultured in α-MEM (minimal essential medium), supplemented with 2 mM of L-glutamine, 50 μg/mL of gentamicin, 10 mM of HEPES, and 10% FBS. CCLP1 cells were cultured in DMEM, supplemented with 10% FBS, 2 mM of L-glutamine, and 50 μg/mL of gentamicin. Human embryonic kidney 293 cells (HEK293FT) from Life Technologies (Grand Island, NY) were cultured in DMEM, supplemented with 10% FBS, 0.1 mM of MEM nonessential amino acids, 6 mM of L-glutamine, 1 mM of MEM sodium pyruvate, penicillin G (100 U/mL), streptomycin (100 μg/mL), and 500 μg/mL of geneticin. Each of the cell lines listed above were cultured under sterile conditions at 37°C with 5% CO_2 in humidified cell culture incubators.

Fluorescent Immunohistochemistry. Anonymous human CCA tissue samples were obtained through the Liver Tissue Cell Distribution System (Minneapolis, MN), which was funded by the National Institutes of Health (contract no. HHSN276201200017C). Paraffin sections were prepared by Anatomic Pathology Research Services at Medical College of Virginia Campus, Virginia Commonwealth University (VCU; Richmond, VA). The 5-μm sections were deparaffinized and rehydrated. Sections were pretreated with a blocking solution containing 8% normal goat serum (Vector Laboratories, Inc., Burlingame, CA), 3% bovine serum albumin (Fisher Scientific, Fair Lawn, NJ), 0.1% cold fish skin gelatin (Electron Microscopy Science, Hatfield, PA), 0.5% Tween 20, and 0.01% Triton X in phosphate-buffered saline (PBS) for 30 minutes. Sections were then incubated with polyclonal rabbit Ab against S1PR2 (EDG5 [H64], sc-25491, 1:100 dilution; Santa Cruz Biotechnology, Inc., Santa Cruz, CA) overnight 4°C, followed by treatment with Alexa Fluor 555–labeled secondary goat anti-rabbit immunoglobulin G Ab (1:200 dilution; Invitrogen Life Science, Carlsbad, CA) for 2 hours at room temperature. After six 10-minute washes in PBS, sections were mounted with VECTASHIELD HardSet Mounting Medium (Vector Laboratories). Negative control sections were processed without primary or secondary Ab to confirm the specificity of primary Ab for its targets. The images of fluorescent immunostaining of S1PR2 were captured using a Zeiss LSM 710 confocal laser scanning microscope (Carl Zeiss MicroImaging, Inc., Thornwood, NY). The 561-nm laser lines were used for sample illumination and a 63×/1.4 n.a. oil immersion lens was used for single photon confocal imaging.

Quantification of Sphingolipids by Mass Spectrometry. Lipids were extracted from cell-culture media or cell pellets of rat BDE1 and BDEsp-TDE_{H10} cells. S1P levels were quantified by liquid chromatography and electrospray ionization-tandem mass spectrometry (4000 QTRAP; AB Sciex, Framingham, MA), as previously described.[19]

RNA Isolation and Quantitative Real-Time Reverse-Transcriptase Polymerase Chain Reaction. Total cellular RNA was isolated using Trizol reagent (QIAGEN, Inc, Valencia, CA) and reverse transcribed into first-strand complementary DNA (cDNA) using the High-Capacity cDNA Reverse Transcription Kit from Life Technologies. Messenger RNA (mRNA) levels of

S1PRs and SphKs were determined by real-time reverse-transcriptase polymerase chain reaction (RT-PCR) using iQTM SYBR Green Supermix reagents and normalized using β-actin or glyceraldehyde 3-phosphate dehydrogenase (GAPDH) as an internal control, as described previously. Primer sequences are shown in Supporting Table 1.

Western Blotting Analysis. Western blotting analysis of total protein in cell lysates from cultured rat and/or human CCA cell lines was carried out as previously described,[17,20] with the following primary Abs purchased from Santa Cruz Biotechnology, Inc. (Santa Cruz, CA): S1PR2 (H64); S1PR3 (H70); ERK1 (C16); ERK-2 (C-14); p-ERK (E-4); Akt1/2/3/ (H-136); and p-Akt1/2/3/ (ser473). S1PR1 (Ab23695) was purchased from Abcam (Cambridge, MA). Protein bands were normalized against β-actin and detected with mouse monoclonal anti-actin Ab (ACTN05) from Thermo Scientific (Wilmington, DE).

Lentiviral Short Hairpin RNA for Down-Regulating S1PR1 and S1PR2. The lentiviral vectors containing the stem loop sequences of short hairpin RNA (shRNA) specifically targeting the rat S1PR2 and scrambled control sequence were a gift from Dr. Karnam S. Murthy of VCU's Department of Physiology and Biophysics. Recombinant lentiviruses were produced by transient transfection of HEK293FT cells with lentiviral shRNA vector, along with package vectors, using FuGene HD transfection reagent, as previously described.[17]

Viable Cell-Counting Assays. Two separate methods were used to assess *in vitro* cell growth in response to bile acid or S1PR2 antagonist. Briefly, under method 1, cells were plated on 48-well plates and cultured overnight in serum-free medium. After specific treatments with bile acids with or without JTE-013 pretreatments, viable cell counts were determined using the Cellometer Vision CBA Analysis System (Nexcelom Bioscience, Lawrence, MA). Under method 2, cells were cultured in 96-well plates in serum-free medium and assayed for viable cell growth using the Cell Counting Kit-8 (CCK-8) from Dojindo Molecular Technologies, Inc. (Rockville, MD). Absorbance readings were made at A_{450nm} with the Victor^3 Multilabel Plate Counter from PerkinElmer (Waltham, MA).

Cell Migration Scratch Assay. Rat BDE-spTDE$_{H10}$ or human HuCCT1 or CCLP1 cells were plated at an initial cell density of 5×10^5 cells per well in six-well culture dishes and then allowed to form a confluent monolayer. After a 24-hour period without serum, the cell monolayer was scratched with a sterile pipette tip (200 μL), washed with serum-free medium to remove floating and detached cells, and then photographed (time 0 hours) under the 10× objective of an Olympus 1X71 microscope (Olympus Corp., Center Valley, PA). Next, cells were pretreated with JTE-013 (10 μM) or dimethylsulfoxide (DMSO) for 1 hour, then treated with TCA (100 μM) or S1P (100 nM). After 48 hours, the wounded area was photographed as described above. Images acquired for each treatment group were further analyzed using IPLab 4.0. imaging software (Scanalytics, Inc., Rockville, MD).

Organotypic CCA Spheroid/"Duct-Like" Growth Model. The 3D organotypic CCA coculture model used in this study has been previously described.[18] Briefly, BDEsp-TDF$_{E4}$ CAFs (initial plating density = 4×10^5 cells) and BDEsp-TDE$_{H10}$ (initial plating density = 8×10^5 cells) were mixed with rat tail type I collagen gel matrix (BD Biosciences) and plated for 1 hour at 37°C in six-well culture plates. Individual gel matrix cocultures were then gently transferred to 60-mm culture dishes and cultured for 24 hours in our standard medium supplemented with 1.0% FBS. At 24 hours, fresh medium with 1.0% FBS containing either TCA (100 μM) or S1P (100 nM), with or without JTE-013, was respectively added to the cultures, with additional medium changes being made every 48 hours over an 8-day treatment period. At the end of this period, individual gel cocultures were fixed in 10% neutral buffered formalin, paraffin embedded, sectioned at 10 μm, and stained with hematoxylin and eosin (H&E). Computational microscopic imaging of the stained tissue sections was then carried out essentially as previously described,[18] and the numbers of CCA spheroid/duct-like structures formed within the 3D gel were then quantified using cellSens imaging software (Olympus). The microscopic density of each CCA structure analyzed was determined using IPLab 4.0 imaging software (Scanalytics).

Cell Invasion Assay. BDEsp-TDE$_{H10}$ cells (1×10^5) were seeded in the Matrigel-coated upper chamber of the BD Biocoat Matrigel Invasion Chamber. The bottom plastic wells were seeded with either BDE-TDF$_{E4}$ cells (5×10^4) or were without cells and maintained in complete media with 1% FBS. BDEsp-TDE$_{H10}$ cells were pretreated with JTE-013 (10 μM) or vehicle DMSO for 1 hour, then treated with TCA (100 μM), S1P (100 nM), or DMSO only and incubated at 37°C for 48 hours. After 48 hours, noninvasive cells were removed from the top surface of the Matrigel-coated insert. The cells that had migrated to the lower surface from the top surface of the insert were fixed with 3.7% paraformaldehyde and stained with 0.1% crystal violet solution. For each replicate

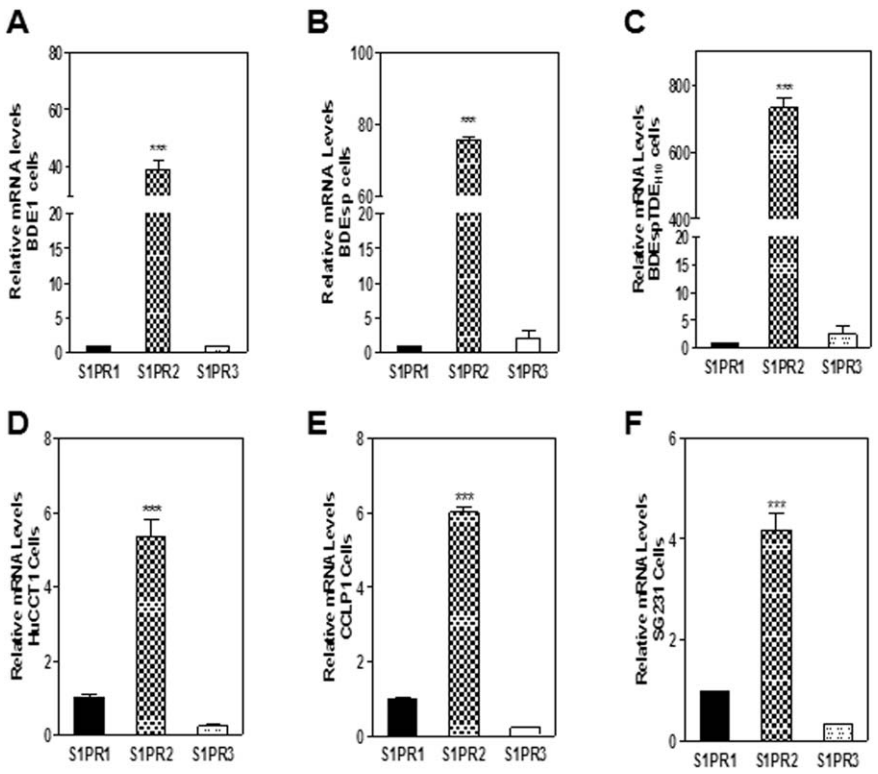

Fig. 1. Differential expression of S1PRs in CCA cells. Total cellular RNA was isolated from (A) rat BDE1, (B) rat BDEsp, (C) rat BDEsp-TDE$_{H10,}$ (D) human HuCCT1, (E) CCLP1, and (F) SG231cells. mRNA levels of individual S1PRs were detected by real-time RT-PCR, as described in Materials and Methods, and normalized using β-actin or GAPDH as an internal control. Relative mRNA levels of S1PR2 and S1PR3 to S1PR1 (designated = 1) are shown. $***P < 0.001$, compared to S1PR1; n = 3.

(n=3), migrated cells were counted and the invasion index was determined according to the manufacturer's instructions, as previously described.[18]

Statistical Analysis. All of the experiments were repeated at least three times, and the results are expressed as mean ± standard deviation. One-way analysis of variance was employed to analyze the differences between sets of data using GraphPad Prism 5.0 (GraphPad Software Inc., San Diego, CA). A *P* value of ≤ 0.05 was considered statistically significant.

Results

S1PR2 Is the Predominant S1PR in CCA. S1P is the natural ligand of the GPCRs, S1PR1-5, which are differentially expressed in different tissues.[21] Previously, we had shown that S1PR2 is highly expressed in the liver and that TCA activates ERK1/2 and Akt through S1PR2 in rat primary hepatocytes.[17] In the current study, we first used real-time RT-PCR to determine the mRNA expression levels of all five S1PRs in both the rat and human CCA cell lines, as well as in nontumorigenic rat BDE1 cholangiocytes. The data shown in Fig. 1 demonstrate S1PR2 to be the dominant S1PR expressed in rat BDE1, BDEsp, and BDEsp-TDE$_{H10}$ cells, as well as in the human HuCCT1, CCLP1, and SG231 CCA cell lines. In contrast, each of these cell lines expressed significantly lower levels of S1PR1 and 3 mRNA, relative to S1PR2 mRNA. Expression of S1PR4 and 5 was not detected in any of the rat and human CCA cell lines tested or in cultured BDE1 cells. In order to determine whether the mRNA expression levels of S1PRs are correlated with the protein levels in CCA cells, we did western blotting analysis. S1PR2 was the predominant S1PR in human HuCCT1, CCLP1 and SG231 CCA cells (Fig. 2A). Similarly, in rat BDEsp-TDE$_{H10}$, S1PR2 expression was significantly up-regulated. To further examine whether S1PR2 expression correlates with the prognosis of CCA, we did immunohistochemistry (IHC) staining of S1PR2 in human CCA tumor tissues and nontumor tissues. S1PR2 expression was significantly higher in CCA tumor tissue than that in nontumor tissue of the same patient (Fig. 2C). These results suggest that the rat BDEsp-TDE$_{H10}$ cell represents an excellent *in vitro* model of human CCA.

Similar to what we found in rat hepatocytes, CBAs also activated ERK1/2 and AKT in BDEsp-TDE$_{H10}$ cells (Supporitng Fig. 1A), and TCA-mediated ERK1/2 and AKT activation was also blocked by JTE-013, a chemical antagonist of S1PR2 (data not shown). More important, we found that TCA and S1P markedly increased nuclear p-ERK1/2 levels, which was completely blocked by JTE-013 (Supporting Fig. 1B), suggesting that S1PR2 activation by CBAs or S1P plays a key role in activating downstream signaling pathways linked to CCA cell growth and migration/invasion.

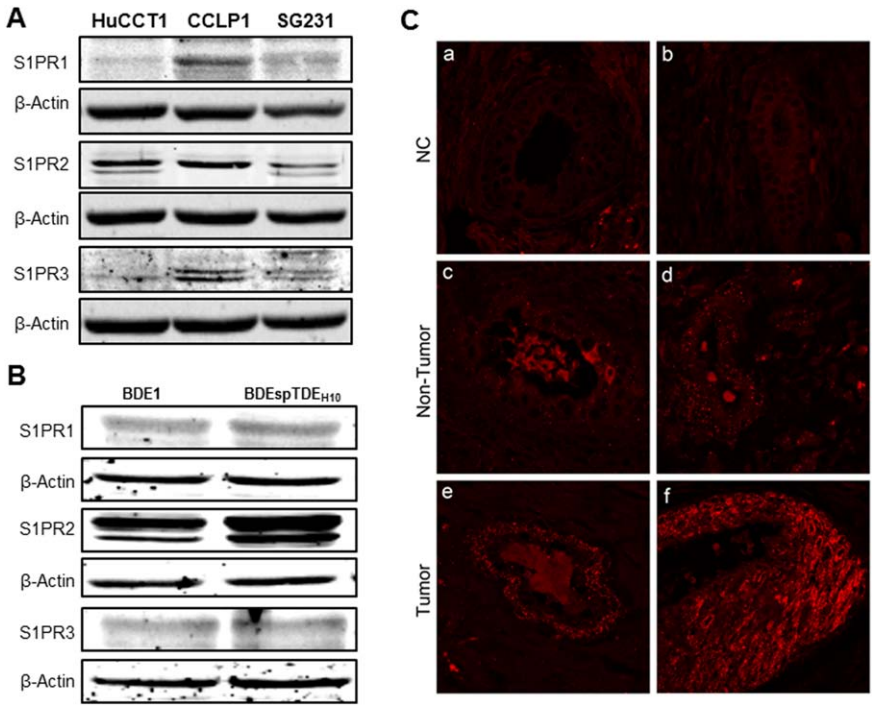

Fig. 2. Differential expression of S1PRs in CCA cells and human CCA tissue. Total cell lysates of (A) human HuCCT1, CCLP1, and SG231 cells and (B) rat BDE1, BDEsp-TDE$_{H10,}$ and BDEsp-TDF$_{E4}$ cells were prepared as previously described.[34] Protein levels of S1PR1, S1PR2, and S1PR3 were determined by western blotting analysis using specific Abs. β-actin was used as loading control. Representative images are shown. (C) Fluorescent IHC staining of S1PR2 in human CCA tissues. Human CCA tumor tissue and nontumor tissue from the same patient were processed for fluorescent IHC staining of S1PR2, as described in Materials and Methods. Representative images are shown. (a) Negative control (NC) without primary and second Ab. (b) NC without primary Ab. (c and d) Nontumor tissues stained with S1PR2. (e and f) Tumor tissues stained with S1PR2.

TCA Induces CCA Cell Growth Through S1PR2 and ERK1/2. Figure 3 and Supporting Fig. 2 demonstrate that TCA, and, to a somewhat lesser extent, GCA, significantly stimulates cell growth in a concentration-dependent manner in both rat BDEsp-TDE$_{H10}$ and human CCLP1 CCA cells, whereas DCA and GDCA had no effect on cell growth. Furthermore, TCA-mediated BDEsp-TDE$_{H10}$ cell growth was significantly inhibited by JTE-013, but JTE-013 alone was also found to be growth inhibitory for these CCA cells in the absence of TCA (Fig. 4A). To confirm the role of S1PR2 in TCA-mediated cell proliferation, we used S1PR2 lentiviral shRNA to specifically silence S1PR2 expression. shRNA knockdown of S1PR2 selectively blocked TCA-mediated cell growth of BDEsp-TDE$_{H10}$ cells, relative to the vehicle control and control shRNA treatments, further suggesting that S1PR2 contributes to CBA-mediated cell proliferation of CCA cells (Fig. 4B). Moreover, TCA-stimulated cell growth of rat BDEsp-TDE$_{H10}$ and human CCLP1 CCA cells in culture was found to be almost completely suppressed by treatment with the MAPK kinase (MEK)1/2 inhibitor, U0126 (Fig. 4C,D). To further elucidate the mechanism underlying the inhibitory effect of JTE-013 alone on cell growth, we measured S1P levels both in culture media and in rat BDE1 and BDEsp-TDE$_{H10}$ cells. BDEsp-TDE$_{H10}$ secreted more S1P in media, compared to BDE1 (Supporting Fig. 3A). But, intracellular S1P level in BDEsp-TDE$_{H10}$ was lower than that in BDE1 cells.

Using a novel 3D coculture model of organotypic CCA growth,[24] we further demonstrated that both TCA and S1P significantly increased the number and size of spheroid/duct-like structures formed from rat BDEsp-TDE$_{H10}$ CCA cells when cocultured with BDEsp-TDF$_{E4}$ CAFs in a rat type I collagen gel matrix (Fig. 5). Similar to our findings shown in Fig. 4A, TCA- and S1P-mediated increases in CCA spheroid number and size was also found to be markedly inhibited by JTE-013, further supporting the role of S1PR2 in CCA cell growth.

Effect of S1PR2 on TCA-Mediated Cell Migration. To determine the effect of TCA on CCA cell migration/invasion and whether S1PR2 is involved in this process, we performed Matrigel invasion assays with rat BDEsp-TDE$_{H10}$ cells (upper chamber) alone or in coculture with BDEsp-TDF$_{E4}$ cells (lower surface) in the presence or absence of TCA or S1P and with or without JTE-013 treatment. TCA (as well as S1P) significantly increased *in vitro* cell migration/invasiveness of BDEsp-TDE$_{H10}$ CCA cells, whereas inhibition of S1PR2 activation by JTE-013 completely blocked TCA-stimulated cell invasion response (Fig. 6D). We also performed *in vitro* scratch (wound) cell migration assays with both rat and human CCA cells, and the results further demonstrated both TCA and S1P to promote CCA cell migration, which also was significantly inhibited by JTE-013 (Fig. 7 and Supporting Figs. 4 and 5).

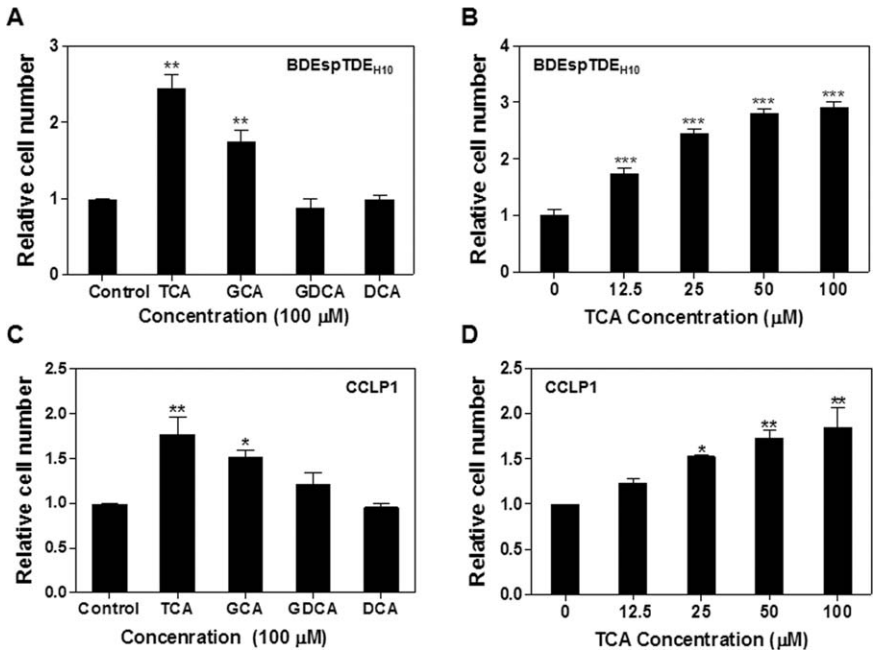

Fig. 3. Effect of bile acids on cell proliferation in CCA cells. Rat BDEsp-TDE$_{H10}$ cells or human CCLP1 cells were serum starved for 24 hours and then treated with individual bile acids, TCA, GCA, GDCA, and DCA at a concentration of 100 μM (A and C) or different concentrations of TCA (0-100 μM) for 48 hours (B and D). At the end of the treatment period, cells were harvested and analyzed using a Cellometer Vision CBA automatic cell counter (Nexcelom Bioscience, Lawrence, MA). Relative cell number, compared to control group, is shown. $^{**}P < 0.01$; $^{***}P < 0.001$, compared to vehicle control; n = 3.

Discussion

Inflammation in the biliary tract together with impaired bile flow are common features of liver diseases, such as PSC, hepatolithiasis, and liver fluke infestation that predispose one for CCA development.[2,22] As further observed in CCA patients, impaired bile flow results in an increased accumulation of CBAs in serum, liver, and bile ducts, as well as

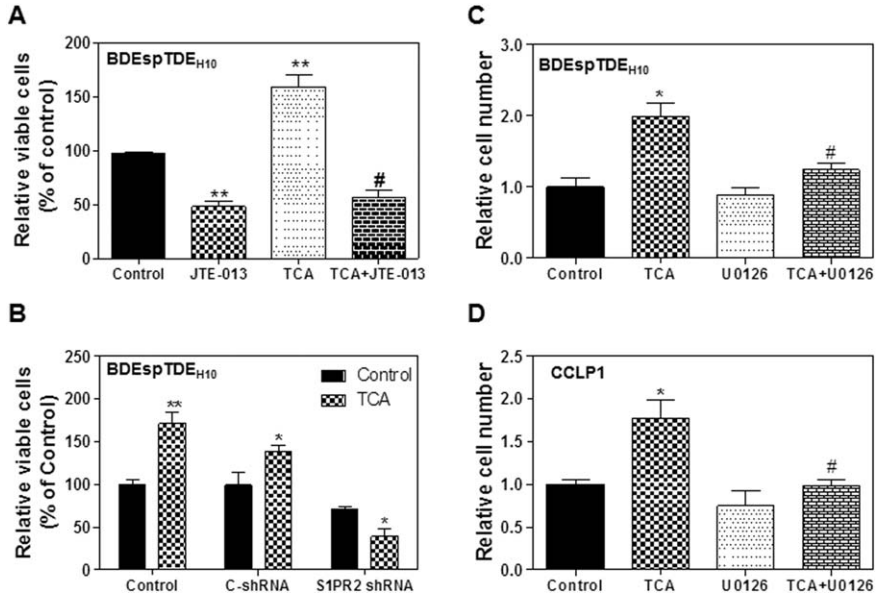

Fig. 4. (A and B) Role of S1PR2 in TCA-mediated cell proliferation in rat BDEsp-TDE$_{H10}$ cells. (A) Cells were plated in serum-free medium for 24 hours and then treated with TCA (100 μM) with or without JTE-013 (10 μM) for 48 hours. At the end of treatment, viable cells were quantified using the CCK-8 kit, as described in Materials and Methods. $^{**}P < 0.01$, compared to vehicle control; $\#P < 0.05$, compared to TCA group; n = 3. (B). Cells were transduced with control or S1PR2 lentiviral shRNA for 24 hours and then treated with control vehicle or TCA (100 μM) for 48 hours. Viable cells were quantified using the CCK-8 kit, as described in Materials and Methods. $^{*}P < 0.05$; $^{**}P < 0.01$, compared to vehicle control; n = 3. (C and D) Effect of ERK1/2 activation on TCA-mediated cell proliferation in CCA cells. Rat BDEsp-TDE$_{H10}$ cells or human CCLP1 cells were serum starved for 24 hours and then treated with vehicle control, TCA (100 μM), the MEK1/2 inhibitor U0126 (10 μM), or TCA plus U0126 for 48 hours. At the end of the treatment period, cells were harvested and analyzed using a Cellometer Vision CBA automatic cell counter (Nexcelom Bioscience, Lawrence, MA). Relative cell number, compared to control group, is shown. (C) BDEsp-TDE$_{H10}$ cells. (D) CCLP1 cells. $^{*}P < 0.05$, compared to vehicle control; $\#P < 0.05$, compared to TCA group; n = 3.

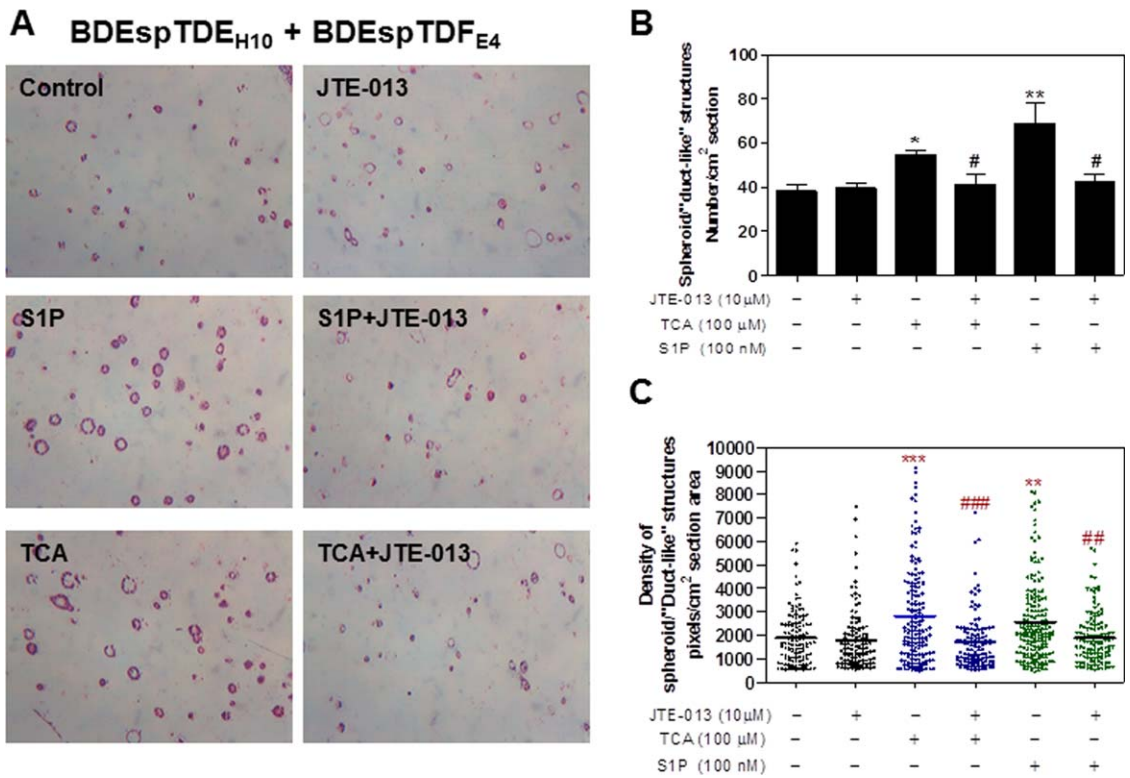

Fig. 5. Effect of TCA and JTE-013 on the expansion of spheroid/"duct-like" structures formed in 3D organotypic cocultures of BDEsp-TDE$_{H10}$ and BDEsp-TDF$_{E4}$ cells. Rat BDEsp-TDE$_{H10}$ and BDEsp-TDF$_{E4}$ cells were mixed with rat-tail type I collagen gel, as described in Materials and Methods. Cells were treated with TCA (100 μM) or S1P (100 nM) with or without JTE-013 (10 μM) for 8 days. At the end of treatment, the collagen gel cultures were fixed and processed for H&E staining. The number and density of spheroid/duct-like structures were quantified as described in Materials and Methods. (A) Representative images of H&E staining of spheroid/duct-like structures formed in vehicle control versus S1P or TCA treatment groups with or without JTE-013. (B) The number of spheroid/duct-like structures/cm^2 for each group was quantified as described in Materials and Methods. *$P < 0.05$; **$P < 0.01$, compared to vehicle control; #$P < 0.05$, compared to TCA or S1P group; n = 3. (C) Density of spheroid/duct-like structures was determined using IPLab4.0. **$P < 0.01$; ***$P < 0.001$, compared to vehicle control; ###$P < 0.001$, compared to TCA group; ##$P < 0.01$, compared to S1P group; n = 3.

lower amounts of unconjugated and secondary bile acids returning from the intestines.[6,23] Moreover, BDO produced by bile duct ligation or by tumor growth in a rat model of CCA progression has been demonstrated to be a potent stimulus for CCA invasive growth and associated increase in gross peritoneal metastases.[4] Based on these observations, we have hypothesized that CBAs may be playing a key role in stimulating CCA cell growth and invasion. However, whereas various mechanisms have been suggested as to how bile acids may be acting to promote CCA, it is still unclear as to how cholestasis leading to an increased accumulation of CBAs in bile might be acting to promote CCA invasive growth.

Our recent findings demonstrated that CBAs, but not free bile acids, activate the ERK1/2- and AKT-signaling pathways through the S1PR2 in rodent hepatocytes in culture and *in vivo*.[17] In the current study, we investigated whether CBA-mediated activation of ERK1/2- and AKT-signaling pathways through S1PR2 provides a novel molecular mechanism for stimulating CCA cell proliferation and cell migration/invasion of human and rat CCA cells. Because activation of the ERK1/2- and AKT-cell signaling pathways has been shown to be important for CCA cell proliferation, invasion, and chemoresistance,[24-26] our findings, which now link CBA-induced cell proliferation and cell migration/invasion to S1PR2 activation and concomitant enhanced phosphorylation of ERK1/2 and AKT in cultured CCA cells, have important implications for understanding how CBAs may be acting to promote CCA-invasive growth.

Specifically, we have shown that (1) both S1PR2 mRNA levels and protein levels are highly expressed in both rat and human CCA cells, (2) S1PR2 is highly expressed in human CCA tissue, compared to nontumor tissue, (3) CBAs activated both the ERK1/2- and AKT-signaling pathways in these cells, with TCA, a very hydrophilic bile acid, being the most potent stimulator of cultured CCA cell growth, (4) *in vitro* cell

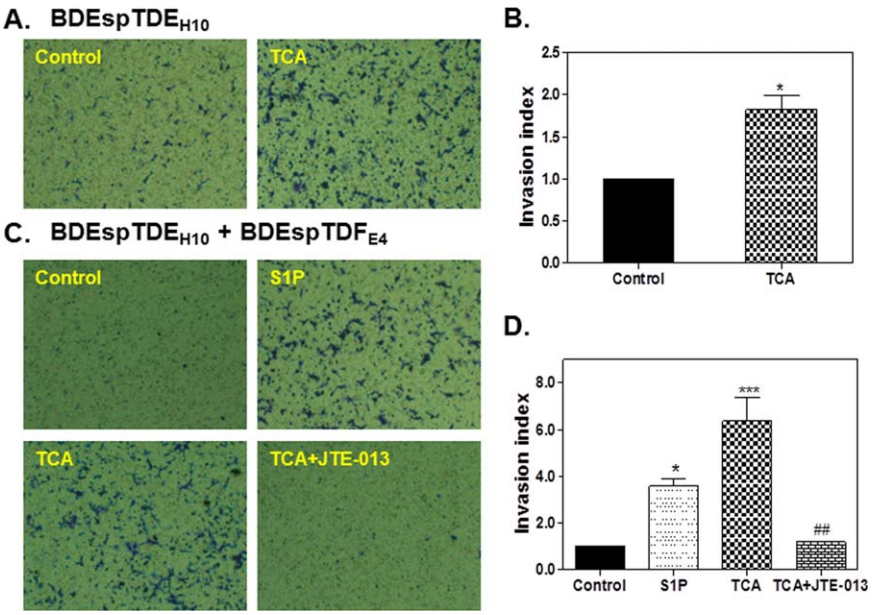

Fig. 6. (A and B) Effect of TCA on cultured BDEsp-TDE$_{H10}$ cell invasion. Rat BDEsp-TDE$_{H10}$ cells were plated in the upper transwell inserts and treated with TCA (100 μM) for 48 hours. At the end of treatment, the number of invasive cells on the lower surface of inserts and invasion index were analyzed as described in Materials and Methods. Representative images for each group are shown. *$P < 0.05$, compared to vehicle control; n = 3. (C and D) Effect of JTE-013 on TCA-induced cell invasion in cultured BDEsp-TDE$_{H10}$ cells. Rat BDEsp-TDE$_{H10}$ cells were plated in upper transwell inserts and pretreated with JTE-013 for 1 hour and then treated with S1P (100 nM) or TCA (100 μM) for 48 hours. At the end of treatment, the number of invasion cells on the lower surface of the inserts and invasion index were analyzed as described in Materials and Methods. *$P < 0.05$; ***$P < 0.001$, compared to vehicle control; ##$P < 0.01$, compared to TCA group; n = 3.

growth stimulation by TCA or S1P was significantly inhibited by a specific chemical antagonist (JTE-013) of S1PR2, as well as by a lentiviral shRNA against S1PR2, (5) JTE-013 was also determined to be a potent inhibitor of TCA- or S1P-stimulated cell migration/invasion of both cultured human and rat CCA cells, and (6) rat CCA cells secrete more S1P than normal cholangiocytes. Taken together, our results strongly suggest that S1PR2 is a key regulator of CCA cell growth stimulation and *in vitro* cell migration/invasion caused by CBAs, which challenges the dogma that S1PR2 is tumor suppressive.[27,28] Although most studies have shown that S1PR1 and S1PR3 are the major S1PRs involved in S1P-mediated cancer cell migration and invasion, the contribution of S1PR2-mediated signaling pathways to cancer cell proliferation and invasion has also been identified in several recent studies.[29-32]

Interestingly, in contrast to TCA, the more hydrophobic bile acids, GDCA and DCA, were largely ineffective in stimulating growth of CCA cells (Fig. 3). It is somewhat unclear why the hydrophilic bile acids stimulate CCA cell growth, whereas the hydrophobic bile acids were without effect. However, we have observed that the steady-state mRNA levels of apical sodium-dependent bile acid transporter (ASBT; or SLC10A2) are markedly down-regulated in both rat and human CCA cells (Supporting Fig. 6). Under normal physiological conditions, CBAs are actively taken up by the ASBT, carried across cholangiocytes, and secreted on the basolateral side by the organic solute transporter (OST)α-OSTβ bile acid transporter.[33] CBAs are known to undergo cholehepatic shunting, which may be involved in regulating important intracellular signaling pathways in cholangiocytes. Thus, it is reasonable to hypothesize that hydrophilic CBAs stimulate CCA cell growth, without entering the cell, by activating the S1PR2 located on the plasma membrane. More highly hydrophobic bile acids may be able to enter CCA cells by simple diffusion and activate intracellular signaling pathways that counteract the effects of S1PR2 activation by external CBAs.

It is also noteworthy that FXR, a putative tumor suppressor in the liver that is highly expressed in the normal human bile duct, but reduced in human CCA tissues,[11] was also found by us to be down-regulated in both human and rat CCA cells, compared with untransformed cholangiocytes (Supporting Fig. 6B). In this context, because free bile acids, but not CBAs, have been shown to up-regulate FXR in CCA cells, it may be that FXR expression is dysregulated as a result of the inability of CBAs to enter CCA cells to up-regulate and activate this nuclear bile acid receptor. Further studies are now needed to investigate the

cellular and molecular relationships between CBA-induced S1PR2 activation and down-regulation of ASBT and FXR in relation to CCA progression.

In the current study, we observed that JTE-013 as well as shRNA against S1PR2 inhibited CCA cell growth in the absence of CBAs (Fig. 3). We have no evidence that JTE-013 is toxic to CCA cells at the concentration (10 μM) used, nor is there any literature reporting that it is toxic to mammalian cells. Here, we hypothesize that secreted S1P generated by SphK1 and 2 may stimulate the growth of CCA cells in an autocrine manner and that JTE-013 may inhibit this process. In this regard, both the rat and human CCA cell lines analyzed in this study were determined to exhibit detectable levels of SphK1 and 2 mRNA, with SphK2 mRNA expression being predominant over that of SphK1 in CCA cells (Supporting Fig. 7). Cancer-associated myofibroblasts (BDEsp-TDF$_{E4}$ cells) derived from orthotopic rat BDEsp CCA stroma were also demonstrated to dominantly express SphK1 mRNA over that of BDEsp-TDE and BDEsp-TDE$_{H10}$ CCA cells isolated from orthotopic BDEsp tumor.[15,17,18] Furthermore, rat BDEsp-TDE$_{H10}$ CCA cells secreted more S1P into media, compared with BDE1 cells (Supporting Fig. 3). Therefore, CCA cells and myofibroblasts may, in part, also be acting to stimulate CCA cells in an auto- and paracrine fashion through secretion of S1P, which activates S1PR2. However, additional studies will be required to further test this hypothesis.

In summary, the current results provide a new explanation for how hydrophilic CBAs promote CCA growth and points to S1PR2 and FXR-α as potentially new therapeutic targets for treating CCA (Fig. 8).

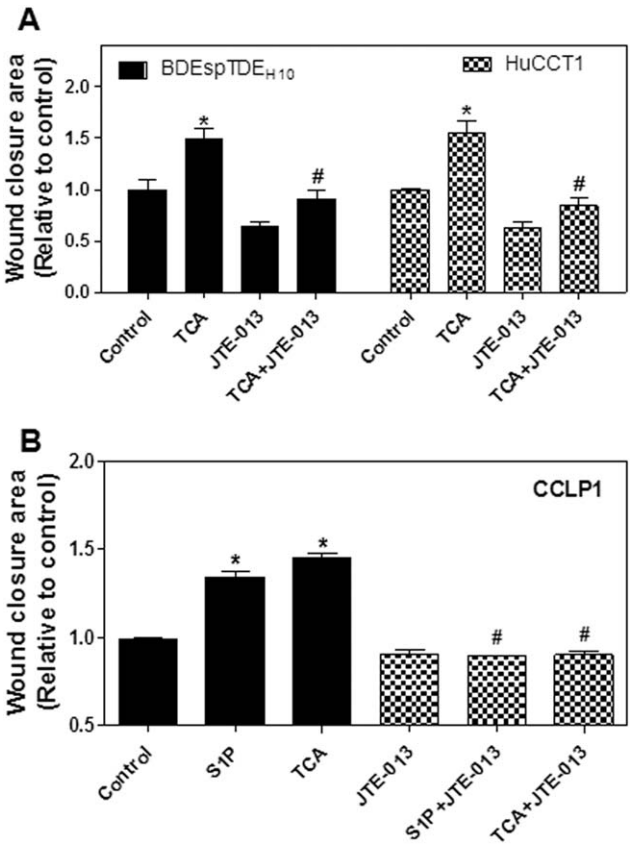

Fig. 7. Effect of S1PR2 activation on CCA cell migration. Rat BDEsp-TDE$_{H10}$ cells, human HuCCT1 cells, and CCLP1 cells were plated on six-well plates until confluent. Cells were scratched to simulate a wound and images were recorded as 0 hours. Cells were pretreated with JTE-013 (10 μM) for 1 hour, then treated with TCA (100 μM) or S1P (100 nM) for 48 hours. Images of wound areas were recorded as described in Materials and Methods. The area of wound was quantified using IPLab4.0. Relative wound closure was calculated. (A) Rat BDEsp-TDE$_{H10}$ cells and human HuCCT1 cells. (B) Human CCLP1 cells. *$P < 0.05$, compared to control group; #$P < 0.05$, compared to corresponding TCA or S1P group, n = 3.

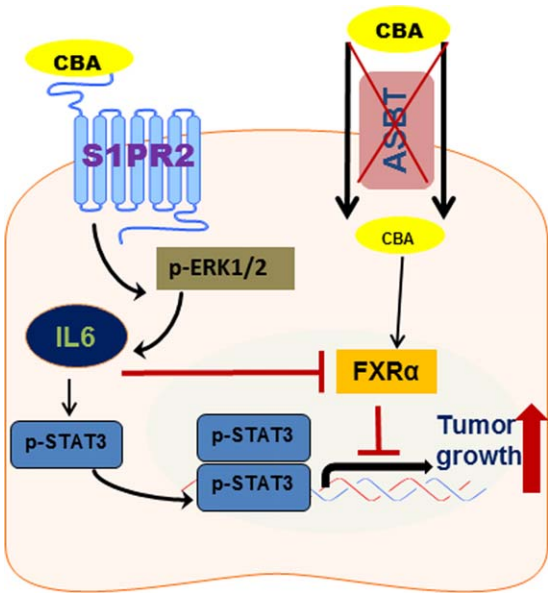

Fig. 8. Schematic diagram of potential mechanisms by which CBAs promote CCA growth. In CCA cells, down-regulation of ASBT prevents CBAs from activating FXR-α. Accumulation of CBAs outside CCA cells will activate ERK1/2-signaling pathways through S1PR2. Activation of ERK1/2 results in the subsequent activation of the IL-6-JAK-STAT3 pathway and stimulates CCA growth. JAK, Janus kinase; STAT3, signal transducer and activator of transcription.

References

1. Welzel TM, Graubard BI, El-Serag HB, Shaib YH, Hsing AW, Davila JA, McGlynn KA. Risk factors for intrahepatic and extrahepatic cholangiocarcinoma in the United States: a population-based case-control study. Clin Gastroenterol Hepatol 2007;5:1221-1228.
2. Razumilava N, Gores GJ. Classification, diagnosis, and management of cholangiocarcinoma. Clin Gastroenterol Hepatol 2013;11:13-21.e11; quiz, e13-14.

3. Sia D, Tovar V, Moeini A, Llovet JM. Intrahepatic cholangiocarcinoma: pathogenesis and rationale for molecular therapies. Oncogene 2013;32: 4861-4870.
4. Sirica AE, Zhang Z, Lai GH, Asano T, Shen XN, Ward DJ, et al. A novel "patient-like" model of cholangiocarcinoma progression based on bile duct inoculation of tumorigenic rat cholangiocyte cell lines. Hepatology 2008;47:1178-1190.
5. Yang H, Li TW, Peng J, Tang X, Ko KS, Xia M, Aller MA. A mouse model of cholestasis-associated cholangiocarcinoma and transcription factors involved in progression. Gastroenterology 2011;141:378-388, 388.e1-4.
6. Jusakul A, Khuntikeo N, Haigh WG, Kuver R, Ioannou GN, Loilome W, et al. Identification of biliary bile acids in patients with benign biliary diseases, hepatocellular carcinoma and cholangiocarcinoma. Asian Pac J Cancer Prev 2012;13(Suppl):77-82.
7. Hashim Abdalla MS, Taylor-Robinson SD, Sharif AW, Williams HR, Crossey MM, Badra GA, et al. Differences in phosphatidylcholine and bile acids in bile from Egyptian and UK patients with and without cholangiocarcinoma. HPB (Oxford) 2011;13:385-390.
8. Dai J, Wang H, Dong Y, Zhang Y, Wang J. Bile acids affect the growth of human cholangiocarcinoma via NF-kB pathway. Cancer Invest 2013;31:111-120.
9. Wu T. Cyclooxygenase-2 and prostaglandin signaling in cholangiocarcinoma. Biochim Biophys Acta 2005;1755:135-150.
10. Meng F, Yamagiwa Y, Ueno Y, Patel T. Over-expression of interleukin-6 enhances cell survival and transformed cell growth in human malignant cholangiocytes. J Hepatol 2006;44:1055-1065.
11. Dai J, Wang H, Shi Y, Dong Y, Zhang Y, Wang J. Impact of bile acids on the growth of human cholangiocarcinoma via FXR. J Hematol Oncol 2011;4:41.
12. Osawa Y, Hannun YA, Proia RL, Brenner DA. Roles of AKT and sphingosine kinase in the antiapoptotic effects of bile duct ligation in mouse liver. Hepatology 2005;42:1320-1328.
13. Kageyama Y, Ikeda H, Watanabe N, Nagamine M, Kusumoto Y, Yashiro M, et al. Antagonism of sphingosine 1-phosphate receptor 2 causes a selective reduction of portal vein pressure in bile duct-ligated rodents. Hepatology 2012;56:1427-1438.
14. Li C, Zheng S, You H, Liu X, Lin M, Yang L, Li L. Sphingosine 1-phosphate (S1P)/S1P receptors are involved in human liver fibrosis by action on hepatic myofibroblasts motility. J Hepatol 2011;54:1205-1213.
15. Dumur CI, Campbell DJ, DeWitt JL, Oyesanya RA, Sirica AE. Differential gene expression profiling of cultured neu-transformed versus spontaneously-transformed rat cholangiocytes and of corresponding cholangiocarcinomas. Exp Mol Pathol 2010;89:227-235.
16. Spiegel S, Milstien S. Sphingosine-1-phosphate: an enigmatic signalling lipid. Nat Rev Mol Cell Biol 2003;4:397-407.
17. Studer E, Zhou X, Zhao R, Wang Y, Takabe K, Nagahashi M, et al. Conjugated bile acids activate the sphingosine-1-phosphate receptor 2 in primary rodent hepatocytes. Hepatology 2012;55:267-276.
18. Campbell DJ, Dumur CI, Lamour NF, Dewitt JL, Sirica AE. Novel organotypic culture model of cholangiocarcinoma progression. Hepatol Res 2012;42:1119-1130.
19. Nagahashi M, Kim EY, Yamada A, Ramachandran S, Allegood JC, Hait NC, et al. Spns2, a transporter of phosphorylated sphingoid bases, regulates their blood and lymph levels, and the lymphatic network. FASEB J 2013;27:1001-1011.
20. Zhou H, Pandak WM, Jr., Lyall V, Natarajan R, Hylemon PB. HIV protease inhibitors activate the unfolded protein response in macrophages: implication for atherosclerosis and cardiovascular disease. Mol Pharmacol 2005;68:690-700.
21. Karimian G, Buist-Homan M, Schmidt M, Tietge UJ, de Boer JF, Klappe K, et al. Sphingosine kinase-1 inhibition protects primary rat hepatocytes against bile salt-induced apoptosis. Biochim Biophys Acta 2013;1832:1922-1929.
22. Al-Bahrani R, Abuetabh Y, Zeitouni N, Sergi C. Cholangiocarcinoma: risk factors, environmental influences and oncogenesis. Ann Clin Lab Sci 2013;43:195-210.
23. Changbumrung S, Tungtrongchitr R, Migasena P, Chamroenngan S. Serum unconjugated primary and secondary bile acids in patients with cholangiocarcinoma and hepatocellular carcinoma. J Med Assoc Thai 1990;73:81-90.
24. Schmitz KJ, Lang H, Wohlschlaeger J, Sotiropoulos GC, Reis H, Schmid KW, Baba HA. AKT and ERK1/2 signaling in intrahepatic cholangiocarcinoma. World J Gastroenterol 2007;13:6470-6477.
25. Menakongka A, Suthiphongchai T. Involvement of PI3K and ERK1/2 pathways in hepatocyte growth factor-induced cholangiocarcinoma cell invasion. World J Gastroenterol 2010;16:713-722.
26. Yoon H, Min JK, Lee JW, Kim DG, Hong HJ. Acquisition of chemoresistance in intrahepatic cholangiocarcinoma cells by activation of AKT and extracellular signal-regulated kinase (ERK)1/2. Biochem Biophys Res Commun 2011;405:333-337.
27. Pyne S, Edwards J, Ohotski J, Pyne NJ. Sphingosine 1-phosphate receptors and sphingosine kinase 1: novel biomarkers for clinical prognosis in breast, prostate, and hematological cancers. Front Oncol 2012; 2:168.
28. Lepley D, Paik JH, Hla T, Ferrer F. The G protein-coupled receptor S1P2 regulates Rho/Rho kinase pathway to inhibit tumor cell migration. Cancer Res 2005;65:3788-3795.
29. Beckham TH, Cheng JC, Lu P, Shao Y, Troyer D, Lance R, et al. Acid ceramidase induces sphingosine kinase 1/S1P receptor 2-mediated activation of oncogenic Akt signaling. Oncogenesis 2013;2:e49.
30. Ikeda H, Watanabe N, Ishii I, Shimosawa T, Kume Y, Tomiya T, et al. Sphingosine 1-phosphate regulates regeneration and fibrosis after liver injury via sphingosine 1-phosphate receptor 2. J Lipid Res 2009;50: 556-564.
31. Li MH, Sanchez T, Milne GL, Morrow JD, Hla T, Ferrer F. S1P/S1P2 signaling induces cyclooxygenase-2 expression in Wilms tumor. J Urol 2009;181:1347-1352.
32. Li MH, Sanchez T, Yamase H, Hla T, Oo ML, Pappalardo A, et al. S1P/S1P1 signaling stimulates cell migration and invasion in Wilms tumor. Cancer Lett 2009;276:171-179.
33. Ballatori N, Christian WV, Lee JY, Dawson PA, Soroka CJ, Boyer JL, et al. OSTalpha-OSTbeta: a major basolateral bile acid and steroid transporter in human intestinal, renal, and biliary epithelia. Hepatology 2005;42:1270-1279.
34. Wu X, Zhang L, Gurley E, Studer E, Shang J, Wang T, et al. Prevention of free fatty acid-induced hepatic lipotoxicity by 18beta-glycyrrhetinic acid through lysosomal and mitochondrial pathways. Hepatology 2008;47:1905-1915.

Supporting Information

Additional Supporting Information may be found in the online version of this article at the publisher's website.